

## NUMERICAL SIMULATION OF THE THREE EDGE BEARING TEST OF STEEL FIBER REINFORCED CONCRETE PIPES

**Facundo L. Ferrado<sup>a</sup>, Mario R. Escalante<sup>a,b</sup> and Viviana C. Rougier<sup>a,b</sup>**

<sup>a</sup>*GIMCE, Facultad Regional Concepción del Uruguay - Universidad Tecnológica Nacional, Ing. Pereyra 676, 3260 Concepción del Uruguay, Argentina, gimce@frcu.utn.edu.ar*

<sup>b</sup>*GEHE, Facultad Regional Concordia - Universidad Tecnológica Nacional, Salta 277, 3200 Concordia, Argentina,*

**Keywords:** Concrete pipes, SFRC, plasticity, nonlineality material.

**Abstract.** Historically, steel has been the material chosen to improve the tensile behaviour of concrete. Nowadays, the trending of replacing the traditional reinforcement bars with short and slender fibers randomly distributed in the mass concrete, is growing. This composite material made essentially of common concrete reinforced with discrete fibers is called steel fiber reinforced concrete(SFRC). In this work the mechanical behaviour of SFRC pipes is studied, simulating the diametral compression test called three edge bearing test by means of a 2d model in plane strain state. The SFRC is considered as a homogeneous material and its behaviour is represented through some damage - plasticity model (concrete damage plasticity) which takes into account the progressive reduction in the values of the elastic constants due to plastic strain and damage by means of a stiffness degradation variable. The model assumes that the main two failure mechanisms of the concrete are tensile cracking and compressive crushing, thus, the tensile and compression response is characterized through differentiated uniaxial stress-strain curves. This representation, although simplified, captures the most important features of the concrete response. The equations are solved with a commercial computational package. In addition, and as an alternative for the same problem, a case is addressed in which the SFRC is considered as an equivalent homogeneous material too, although a coupled plastic-damaged model is used where the coupling between plasticity and damage is achieved through a simultaneous solution of the plastic and the damage problem. Finally is presented a modified coupled damaged plasticity model that comes from a modification of the Lubliner-Oller yield criterion from the adoption of a yield function of second degree in the components of the stress tensor. For the coupled damage plasticity the contribution of the fibers is considered through the classic mixture theory according to it is performed a modification of the elastic constants depending on the volumetric contribution of the fibers. Here, the problem is solved using the non-linear finite elements code PLastic Crack dynamic (PLCd) The validity of the numerical tool is performed comparing the results of the simulation with experimental data existing in the literature.

## INTRODUCTION

Since the beginning of the 1960s, there has been significant progress in the research on fibre-reinforced concrete, and present, fibres of various kinds are being used to reinforce concrete in structural applications. Due to its high stiffness, the steel fibre reinforced concrete (SFRC) is probably the most commonly used fibre material. ([Kiranbala and Bishwotrij, 2013](#))

Nowadays, it is well stated that one of the most important properties of steel fibre reinforced concrete (SFRC) is its higher resistance to cracking and crack propagation. As a result of their ability to arrest cracks, fibre composites have increased extensibility and tensile strength, both at the first crack and at last, particularly under flexural loading. Also, the fibres are able to hold the matrix together even after extensive cracking. The net result of all these is to provide the fibre composite with pronounced post-cracking ductility and an increase in the toughness of the concrete (defined as some function of the area under the load vs. deflection curve), under any type of loading. That is, the fibers tend to increase the strain at peak load, and provide a great deal of energy absorption in the post-peak portion of the load vs. deflection curve. ([Vaigarade and Bhedi, 2015](#))

## 1 SFRC IN PIPES

Concrete and reinforced-concrete pipes have been in widespread use for the conveyance of storm water and sewage water, and even for irrigation water as low pressure conduits since the late 1800s. In recent decades, many applications of steel-fibre concrete have been found such as tunnel linings, factory floors, and concrete pipes. The use of fibers in the manufacturing of concrete pipes provides significant advantages from a structural and economic point of view. From the former, as previously mentioned, a substantial improvement of many mechanical properties of the concrete are achieved (ductility, toughness). Likewise, in the case of a combination between steel bars and steel fibers, a positive structural synergy is observed: the bars develop the principal resistant function while the fibers realize a sew effect over the cracks reducing its separation and width and, in addition, it collaborates with the resistant function. From the economic point of view, the diminution or elimination of the use of steel bars for the manufacturing of the reinforcement cage, results in a diminution of mounting operations, machinery and associated risks ([de la Fuente et al., 2010](#)). Figure 1 shows an image of the moulding and vibrating process of the pipes along with a picture of the surface finishing.



Figure 1: a) moulding and vibrating process b) surface finishing

However, it should be mentioned that another relevant aspect related to the technology of SFRC pipes is the lack of simplified calculation methods. Because of this, the design of SFRC pipes is normally carried out by trial and error: trying out several dosages of fibres until finding an optimal value that satisfies the requirements of a desired strength class. This design procedure is operationally difficult and uneconomical due to the variety of internal diameters, wall thickness, strength classes and types of fibres. For this reason, it is necessary to develop analytical and/or numerical tools that would make it possible to carry out the optimal design and the verification of the pipes.([de la Fuente et al., 2014](#))

## 2 GENERALITIES OF MIX DESIGN AND PRODUCTION OF SFRC

The addition of steel fibers to concrete require an alteration to the mix design to compensate the loss of workability due to the extra paste needed for coating the surface of the added steel fibers. While many technical and economical advantages are benefited from using SFRC, drawbacks can also be found. However, they are not likely to cause major problems.

As with any other type of concrete, the mix proportions for SFRC depend on the requirements for a particular job, in terms of strength, workability, and so on. Several procedures for proportioning SFRC mixes are available, which emphasize the workability of the resulting mix. However, there are some considerations that are specific to SFRC:

- In general, SFRC mixes contain higher cement contents and higher ratios of fine to coarse aggregate than ordinary concretes, and so the mix design procedures applicable to conventional concrete may not be entirely suitable for SFRC.
- To improve the workability of higher fibre volume mixes, water reducing admixtures and, in particular, superelasticizers are often used, in conjunction with air entrainment.
- The second factor which has a major effect on workability is the aspect ratio ( $l/d$ ) of the fibres. The workability decreases with increasing aspect ratio. In practice it is very difficult to achieve a uniform mix if the aspect ratio is greater than 100.

When SFRC is produced for a certain purpose, the basic problem is to introduce a sufficient volume of uniformly dispersed fibers to achieve the desired improvements in mechanical behaviour, while retaining sufficient workability in the fresh mix to allow proper mixing.

The other main difficulty at the moment of produce SFRC is obtaining a uniform fibre distribution due to the tendency for steel fibres to ball or clump together. In order to avoid this, care should be taken during the mixing procedures, e.g. not adding the fibers too quickly and putting them last to the wet concrete). ([Van Chahn, 2001](#))

## 3 MODELLING OF SFRC

Certain properties of SFRC and most building materials in general can be assessed by means of constitutive models which are just mathematical simplifications of a quite complex physical behavior, and there is no such thing as an “exact” model.

In addition to the experimental investigation, large efforts have been devoted to the analysis and modelling of fibrous materials on the material as well as on the structural level. Typically, a phenomenological approach is adopted, where the enhanced ductility of SFRC is taken into

account by means of a modification of the softening law in plain concrete models. ([Zhan et al., 2014](#))

### 3.1 Model used

Constitutive modelling of concrete materials has been a theme of research for some decades. Nevertheless, the complex behaviour of concrete, due to its composite nature, cannot always be faithfully reflected in any models dedicated to the constitutive modelling of the material ([Nguyen, 2005](#)).

The task of the engineer is to choose a model that is sufficiently accurate and not too complex and computationally expensive ([Roussel, 1996](#)).

In this work, two different models are used for the study of the mechanical behavior of the SFRC.

### 3.2 Concrete damage plasticity

This model is a continuum, plasticity-based, and damage model for concrete. It assumes that the main two failure mechanisms are tensile cracking and compressive crushing of the concrete material. The evolution of the yield (or failure) surface is controlled by two hardening variables (as tensile and compressive equivalent plastic strains) linked to failure mechanisms under tension and compression loading, respectively. In the following, the main assumptions about the mechanical behavior of concrete are exposed:

- Uniaxial response: The model assumes that the uniaxial tensile and compressive response of concrete is characterized by damaged plasticity, as shown in Figure 2.

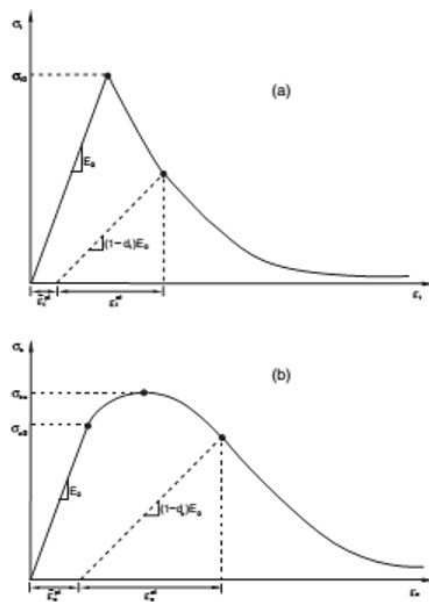


Figure 2: Response of concrete to uniaxial loading in tension (a) and compression (b)

Under uniaxial tension the stress-strain response follows a linear elastic relationship until the value of the failure stress  $\sigma_{t0}$  , is reached. The failure stress corresponds to the on-

set of micro-cracking in the concrete material. Beyond the failure stress the formation of micro-cracks is represented macroscopically with a softening stress-strain response, which induces strain localization in the concrete structure. Under uniaxial compression the response is linear until the value of initial yield,  $\sigma_{c0}$ . In the plastic regime the response is typically characterized by stress hardening followed by strain softening beyond the ultimate stress,  $\sigma_{cu}$ . This representation, although somewhat simplified, captures the main features of the response of concrete.

As shown in Figure 2, when the concrete specimen is unloaded from any point on the strain softening branch of the stress-strain curves, the unloading response is weakened: this means that the elastic stiffness of the material appears to be damaged (or degraded). The degradation of the elastic stiffness is characterized by two damage variables  $d_c$  and  $d_t$ . The damage variables can take values from zero, representing the undamaged material, to one, which represents total loss of strength.

- Tension stiffening: The postfailure behavior is modeled with tension stiffening, which allows you to define the strain-softening behavior for cracked concrete. This behavior also allows for the effects of the reinforcement interaction with concrete to be simulated in a simple manner. Tension stiffening is required in the concrete damaged plasticity model.

In reinforced concrete the specification of postfailure behavior generally means giving the postfailure stress as a function of cracking strain. The cracking strain is defined as the total strain minus the elastic strain corresponding to the undamaged material.

- Compressive behavior: the stress-strain behavior of plain concrete in uniaxial compression outside the elastic range can be defined. Compressive stress data are provided as a tabular function of inelastic (or crushing) strain. Hardening data are given in terms of an inelastic strain instead of plastic strain. The compressive inelastic strain is defined as the total strain minus the elastic strain corresponding to the undamaged material.
- Plastic flow: The concrete damaged plasticity model assumes nonassociated potential plastic flow. The flow potential  $G$  used for this model is the Drucker-Prager hyperbolic function:

$$G = \sqrt{(\epsilon\sigma_{t0} \tan \psi)^2 + q^2} - p \tan \psi \quad (1)$$

where:

$p$  = hydrostatic pressure stress tensor.

$q$  = equivalent Mises stress tensor.

$\psi$  = dilation angle measured in the tensile meridian.

$\sigma_{t0}$  = is the uniaxial tensile stress at failure.

$\epsilon$  = is a parameter, referred to as the eccentricity, that defines the rate at which the function approaches the asymptote (the flow potential tends to a straight line as the eccentricity tends to zero).

- Yield function: The model makes use of the yield function of Lubliner et. al. (1989) ([Lubliner et al., 1989](#)), with the modifications proposed by Lee and Fenves (1998) ([Lee](#)

and Fenves, 1998) to account for different evolution of strength under tension and compression. In terms of effective stresses, the yield function takes the form:

$$F = \frac{1}{1-\alpha} (q - 3\alpha p + \beta(\epsilon_c^{pl})(\sigma_{max}) - \gamma(-\sigma_{max})) - (\sigma_c(\epsilon_c^{pl})) = 0 \quad (2)$$

with:

$$\begin{aligned} \alpha &= \frac{\frac{\sigma_{b0}}{\sigma_{c0}} - 1}{2\frac{\sigma_{b0}}{\sigma_{c0}} - 1}; 0 < \alpha < 0.5 \\ \beta &= \frac{\sigma_c(\epsilon_c^{pl})}{\sigma_t(\epsilon_t^{pl})}(1 - \alpha) - (1 + \alpha) \\ \gamma &= \frac{3(1 - K_c)}{2K_c - 1} \end{aligned}$$

where  $\sigma_{max}$  is the maximum principal effective stress,  $\sigma_{b0}/\sigma_{c0}$  is the ratio of initial equibiaxial compressive yield stress to initial uniaxial compressive yield stress (the default value is 1.16),  $K_c$  is the ratio of the second stress invariant on the tensile meridian,  $\sigma_t$  is the effective tensile cohesion stress, and  $\sigma_c$  is the effective compressive cohesion stress.

### 3.3 Coupled damage plasticity model

Like all geomaterial, concrete when subjected to mechanical forces, exhibit nonlinear behavior characterized by the development of permanent deformation and stiffness degradation. The appearance of permanent deformations can be associated with the development of microcracks, while the stiffness degradation is caused by changes in the porous structure of the concrete. The theories of plasticity and damage can be used as a mathematical framework for describing these phenomena.

The model presented in this paper is thermodynamically consistent and comes from a generalization of plasticity theory and isotropic damage theory. Coupling of damage and plastic strains is achieved by solving both problems simultaneously. In this way correct energy dissipation is also assured (Luccioni et al., 1996).

#### 3.3.1 Plastic process

The plastic process is described from a generalization of the classical theory of plasticity that allows to consider some aspects of the behavior of geomaterials. The behavior of the elastic limit is set by a yield function which marks the beginning of the permanent deformation:

$$F^p(\sigma_{ij}; \kappa^p) = f^p(\sigma_{ij} - K^p(\sigma_{ij}; \kappa^p)) \leq 0 \quad (3)$$

where  $f^p(\sigma_{ij})$  is the equivalent stress defined in the stresses space that could take the form of any of the yield criterion of the classic plasticity (Tresca, Von Mises, Mohr Coulomb, Drucker Prager, etc.). If this model is used for concrete an appropriate criterion for friction materials should be adopted, in this case the Lubliner Oller criterion (Lubliner et. al. 1989) is used.

$K^p(\sigma_{ij}; \kappa^p)$  is the yield threshold and  $\kappa^p$  is the plastic damage variable or isotropic hardening variable. The following evolution rule for the plastic strains is defined:

$$\epsilon_{ij}^p = \lambda \frac{\delta G(\sigma_{mn}; \kappa^p)}{\delta \sigma_{ij}}. \quad (4)$$

Where  $\lambda$  is the plastic consistency factor and  $G$  is the potential function.

The variable plastic hardening is obtained by dividing the energy dissipated by the total energy (area under the curve  $\sigma - e^p$ ). This varies between 0 for virgin material and 1 when it has been plastically dissipated all the energy which the material is capable of dissipating in this way. It is proposed for it, the following rule of evolution that takes into account the different behavior in tension and compression and can adequately simulate the energy dissipation in concrete:

$$\kappa^p = \left[ \frac{r}{g_f^{*p}} + \frac{1-r}{g_c^{*p}} \right] \sigma_{ij} \dot{\epsilon}_{ij}^p \quad (5)$$

where:

$$r = \frac{\sum_{i=1}^3 < \sigma_i >}{\sum_{i=1}^3 \sigma_i}, \quad < \sigma_i > = \frac{1}{2} [\sigma_i + |\sigma_i|] \quad (6)$$

$$g_f^{*p} = \left( \frac{\sum_{i=1}^3 |\sigma_i| R^{op}}{f^p(\sigma_{ij})} \right) g_f^p \quad g_c^{*p} = \left( \frac{\sum_{i=1}^3 |\sigma_i|}{f^p(\sigma_{ij})} \right) g_c^p \quad (7)$$

being  $\sigma_i$  the principal stresses and  $R^{op}$  the relation between the yielding threshold in uniaxial compression and that corresponding to uniaxial tension;  $g_f^p$  and  $g_c^p$  are the maximum energy densities dissipated by the plastic process in uniaxial tension and compression processes, respectively.

The following evolution equation is proposed for the equivalent yielding threshold:

$$K^p(\sigma_{ij}; \kappa^p) = r R^{op} \sigma_t(\kappa^p) + (1-r) \sigma_c(\kappa^p). \quad (8)$$

Where  $\sigma_t(\kappa^p)$  y  $\sigma_c(\kappa^p)$  represents the evolution of the yield threshold in tension and compression uniaxial tests respectively, while  $R^{op}$  is the ratio between the yield thresholds in uniaxial compression and uniaxial tension.

### 3.3.2 Damage process

Now considering the damage process, and in analogous manner to the limit of plastic behavior, a limit or threshold damage is defined, which is described by a function with the following form:

$$F^d = f^d(\sigma_{ij} - K^d(\sigma_{ij}); \kappa^d) \leq 0. \quad (9)$$

Similarly to that seen in the plastic process  $f^d(\sigma_{ij})$  is the equivalent stress defined in the stresses space,  $K^d(\sigma_{ij}, \kappa^d)$  is the equivalent threshold damage and  $\kappa^d$  is the hardening damage variable.

The hardening damage variable varies between 0 for the virgin material to 1 for the material completely damaged. It is obtained normalizing the dissipated energy by damage to the unity.

$$\kappa^d = \left[ \frac{r}{g_f^{*d}} + \frac{1-r}{g_c^{*d}} \right] \psi_0 d \quad (10)$$

$$g_d^{*p} = \left( \frac{\sum_{i=1}^3 |\sigma_i| R^{od}}{f^d} \right) g_f^d \quad g_c^{*d} = \left( \frac{\sum_{i=1}^3 |\sigma_i|}{f^d} \right) g_c^d \quad (11)$$

The following equation for the equivalent damage threshold is proposed:

$$K^d(\sigma_{ij}; \kappa^d) = r\sigma_t(\kappa^d) + (1-r)\sigma_c(\kappa^d), \quad (12)$$

where  $\sigma_t(\kappa^d)$  y  $\sigma_c(\kappa^d)$  represents the evolution of the thresholds damage in uniaxial tension and compression respectively.

### 3.3.3 Coupled plastic-damage response

The evolution of the plastic strains and damage is obtained from the simultaneous solution of the following equations named problem consistency conditions:

$$\begin{cases} F^p = 0 \\ F^d = 0 \end{cases}. \quad (13)$$

These consistency equations are two lineal equations in  $\lambda$  and  $\delta$  that can be easily solved.

## 3.4 Modified coupled damage plasticity model

Here, an adaptation of plasticity model and coupled damage above-mentioned is shown. The extension of the model is achieved by modifying the terms of the variables of hardening and adopting a yield function of second degree in the components of the stress tensor. For this reason, in this modified criterion, maximum traction meridians and maximum compression meridians are curved rather than straight, and a non-isotropic hardening occur which allows to obtain numerical results closer to the experimental values for the type of solicitation studied here.

In the original coupled plasticity damage model, factors in brackets in equations (7) appear high to the first power. In this adaptation, these factors appear high to the second power which can increase the energy dissipation capacity. The same applies to factors in brackets in equations (12) corresponding to damage process (Luccioni and Rougier, 2005).

### 3.4.1 Yield function

The yield criterion used in this model is a modification of the yield criterion of Lubliner-Oller (Lubliner et. al., 1998) with straight meridians. The latter criterion, uses first degree homogeneous flow functions in the components of the stress tensor. In order to better fit the experimental observations, the following expression for the yield function is proposed, in which a second-degree term is introduced in the first invariant of the stress tensor:

$$F^p = \sqrt{3J_2} + \alpha I_1 + \beta(\sigma^{max}) - \gamma(-\sigma^{max}) + \frac{\delta}{\sigma_c(\kappa^p)}(1-\alpha)I_1^2 - \sigma_c(\kappa^p)(1+\alpha)(1+\delta) \leq 0, \quad (14)$$

where  $\alpha$ ,  $\beta$  and  $\gamma$  are constants that determine the shape of the yield function,  $I_1$  is the first invariant of the stress tensor,  $J_2$  is the second invariant of the deviatoric stress tensor,  $\sigma_{max}$  is the greatest principal stress:  $\sigma_3 \leq \sigma_2 \leq \sigma_1 = \sigma_{max}$ , whose expression is:

$$\sigma_{max} = 2 \frac{\sqrt{J_2}}{\sqrt{3}} \sin(\theta + \frac{2\phi}{3}) + \frac{I_1}{3}, \quad (15)$$

where  $\theta$  is the angle of similarity or Lode angle.

## 4 FINITE ELEMENT MODELLING OF THE THREE EDGE BEARING TEST

A 2D model was performed to simulate the test. The test is called three edge bearing test and consists of a diametral compression test which is used to classify the pipes in five strength classes. A line load was applied along the crown of the pipe using universal displacement controlled testing system. The arrangement of the load and the supports are the specified by the ASTM C497 standard and are depicted in Figure 3.

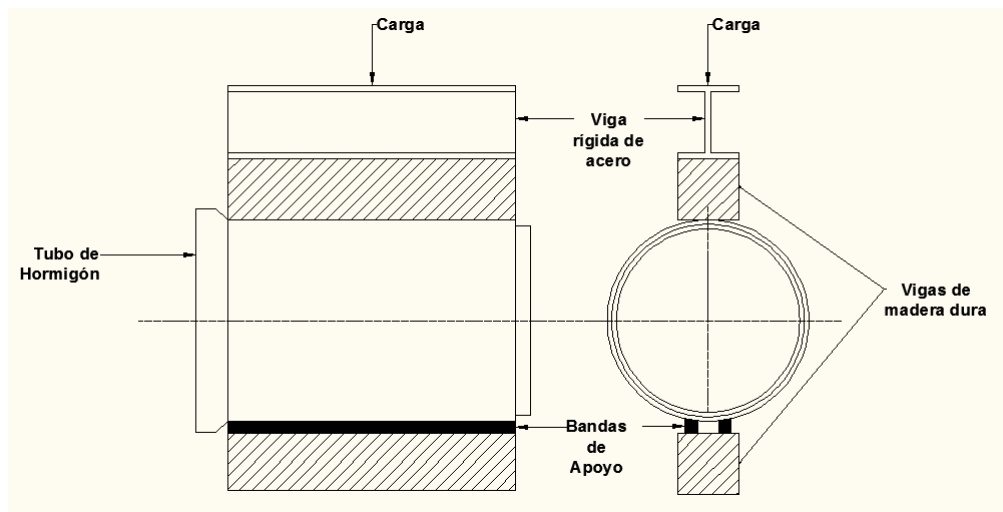


Figure 3: Set up of Three Edge Bearing Test according to ASTM C497

Figure 4 shows the proposed model and the mesh. Lower supports were modeled as rigid elastic and are fixed at the bottom to prevent movement or rotation. Displacement controlled loading was accomplished by applying a 20 mm downward displacement at the upper bearing strip.

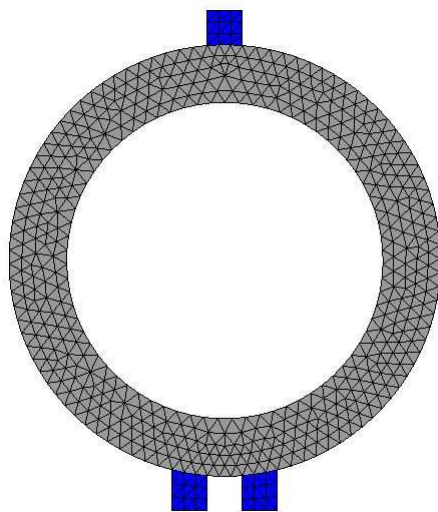


Figure 4: Finite element mesh and model used

The upper loading support, two lower supporting strips and the concrete pipe were modeled. The supports are 50mm wide and 50mm high and the spacing between them is 50 mm. Studied pipes have an internal diameter of 450 mm and a wall thickness of 82mm. The pipe was modeled using 3-node linear triangular elements in plane strain state.

Two mixtures were studied: both have the same dosage of fibers ( $30\text{kg}/\text{m}^3$ ) but were made from two different types of fibers, which we will call hereafter as long fibers and short fibers. Mixtures are called as SL30 (long fibers) and SS30 (short fibers).

Figure 5 shows a diagram of stresses in direction of the coordinate axes. The simulation shows an agreement with the typical stress distribution for this type of test, in which the highest tensile stresses are concentrated on the outer part of the tube.

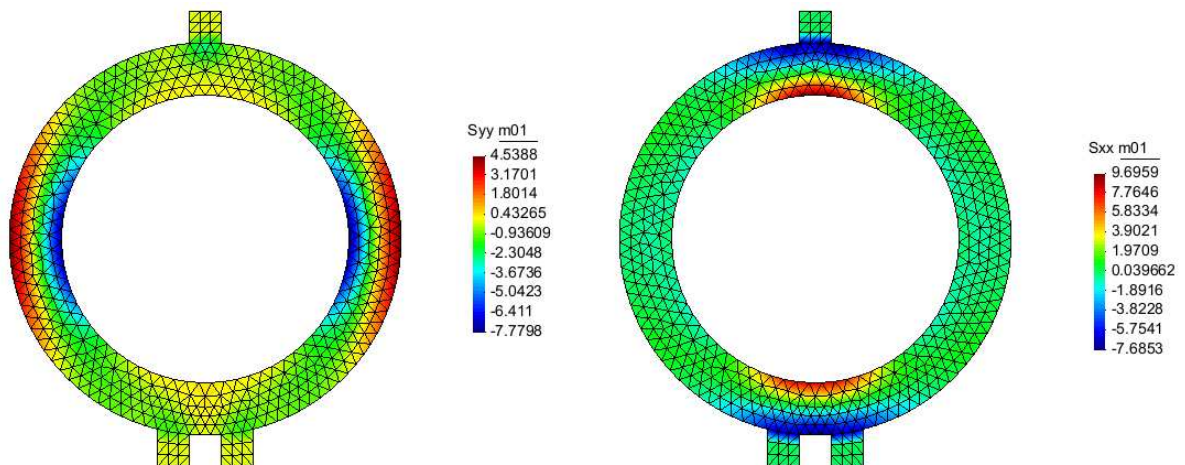


Figure 5: Stress distribution diagram

The parameters required by the concrete damage plasticity model were obtained from the work of another author ([Mohamed, 2015](#)) including uniaxial tension and compression stress-strain curves. The table 1 shows the parameters used in the concrete damage plasticity model.

Young Modulus (Mpa)	34500
Poisson's Ratio	0.3
Dilation angle	36.51
Flow potential eccentricity	0.1
$\frac{\sigma_{b0}}{\sigma_{c0}}$	1.16
$K_c$	0.67
Viscosity parameter	0
Fluence criterion	Lubliner - Oller modified by Lee and Fenves
Potencial criterion	Lubliner - Oller modified by Lee and Fenves

Table 1: Properties of the mixes and parameters used in the concrete damage plasticity model

For coupled damage plasticity models, the data were extracted from the aforementioned work too, while the missing properties were found by means of the rule of mixtures. These idealizations are not always true for heterogeneous materials as SFRC, for that reason their use in design should be used with extreme caution ([Roylance, 2008](#)). The Table 2 shows the properties of each mix used in this models.

Mix	SS30	SL30
Young Modulus (Mpa)	36.45	36.45
Poisson's Ratio	0.2	0.2
Compression ultimate strength(MPa)	51.54	50.78
Tension ultimate strength (MPa)	11.49	10.72
Yield threshold (Mpa)	38.65	38.08
Fracture energy (N/mm)	6	6
Crushing energy (N/mm)	365.5	365.5
Fluence criterion	Lubliner - Oller / Lubliner-Oller with curved meridians	
Potential criterion	Lubliner - Oller / Lubliner-Oller with curved meridians	

Table 2: Mixes properties used in coupled damage plasticity models

To analyze the validity of the numerical tool, the ultimate loads obtained using the different models were compared with the experimental ones found by the mentioned author. Table 3 shows the numerical and experimental results for each of the two samples studied.

As is observed, the values numerically obtained are very similar for the first two models used here. While for the coupled damaged plasticity model with curved meridians, higher loads and closer to the experimental ones were obtained. As a next step, it is suggested to analyze other mixtures with different fiber dosage and pipes with different dimensions.

Mix	Model Used	Ult. Load (KN)	Exp. Ult. Load (KN)
SS30	Concrete damage plast.	194	
	Coupled damage plast. (straight meridians)	203	256
	Coupled damage plast. (curved meridians)	261	
SL30	Concrete damage plast.	199	
	Coupled damage plast. (straight meridians)	192	273
	Coupled damage plast. (curved meridians)	257	

Table 3: Ultimate loads according experimental tests and numerical model

It is said here that although these models contemplate the damage process , this mechanism was not activated in the simulation of this test.

## 5 CONCLUDING REMARKS

In this work, a numerical simulation of the three edge bearing test for assesing the mechanical behavior of concrete pipes was performed. It is used a 2d model in plain strain state where the SFRC was modeled as a homogeneous material.

From the results obtained it is said that the results obtained by means of the modified coupled damage plasticity have the better correlation with the experimental ones.

As a next stage, the use a more complex 3D model which allows to obtain more certainties about the reliability of this models for the simulation of this test.

## REFERENCES

- ASTMC497. Standard test methods for concrete pipe, manhole sections or tile. 2013.
- de la Fuente A., Aguado A., and Molins C. Diseño óptimo integral de tubos de hormigón. *Hormigón y acero - Asociación Científico-técnica del hormigón estructural*, 61(259), 2010.
- de la Fuente A., Figueiredo A., and Aguado A. Substituting the traditional reinforcement in concrete pipes by using structural fibres. *Concrete plant international*, 5:146–150, 2014.
- Kiranbala D. and Bishwotrij S. Effects of steel fibres in reinforced concrete. *International Journal of Engineering Research & Technology (IJERT)*, 2(10):2906–2913, 2013.
- Lee J. and Fenves G. Plastic damage model for cyclng loads of concrete structures. *Journal of engineering mechanics*, 124(892-900), 1998.
- International Center for Numerical Method in Engineering (CIMNE) & Department of Structures Strength of Materials of the Technic University of Catalonia (UPC). Plastic crack dynamic (plcd). 1998.
- Lubliner J., Oliver J., Oller S., and O E. A plastic-damage model for concrete. *International Journal of solids and structures*, 25(3):299–326, 1989.

- Luccioni B., Oller S., and Danesi R. Coupled plastic-damaged model. *Computer methods in applied mechanics and engineering*, 129:81–89, 1996.
- Luccioni B. and Rougier V. A plastic damage approach for confined concrete. *Computers & Structures*, 83:2298–2256, 2005.
- Mohamed N. *Experimental and numerical study on full-scale precast steel fibre-reinforced concrete pipes*. Ph.D. thesis, The university of western Ontario, 2015.
- Nguyen G. *A Thermodynamic Approach to Constitutive Modelling of Concrete using Damage Mechanics and Plasticity Theory*. Ph.D. thesis, University of Oxford, 2005.
- Roylance D. *Mechanical Properties of Materials*. MIT, 2008.
- Runesson K. Constitutive modeling of engineering materials - theory and computation. Technical Report, Dept. of Applied Mechanics, Chalmers University of Technology, Goteborg, 1996.
- Vaigarade L. and Bhedi V. Comparison of strength between steel fiber reinforced concrete and conventional concrete. *International Journal on Recent and Innovation Trends in Computing and Communication*, 3(2):5–10, 2015.
- Van Chahn N. Steel fiber reinforced concrete. Technical Report, Faculty of Civil Engineering, Ho Chi Minh City University of Technology, 2001.
- Zhan Y., Bui H., Ninic J., Mohseni S., and G. M. Numerical modeling of steel fibre reinforced concrete on the meso- and macro-scale. *Computational Modelling of Concrete Structures*, 2014.